Published OnlineFirst March 29, 2019; DOI: 10.1158/1535-7163.MCT-18-1122

Cancer Biology and Translational Studies

Molecular Cancer Therapeutics

Prospective Clinical Sequencing of Adult Glioma

Siyuan Zheng[1,2,3], Kristin Alfaro-Munoz[1], Wei Wei[4], Xiaojing Wang[3], Fang Wang[5], Agda Karina Eterovic[6], Kenna R. Mills Shaw[6], Funda Meric-Bernstam[6], Gregory N. Fuller[7], Ken Chen[5], Roel G. Verhaak[1,2,5,8], Gordon B. Mills[6], W.K. Alfred Yung[1], Shiao-Pei Weathers[1], and John F. de Groot[1]

Abstract

Malignant gliomas are a group of intracranial cancers associated with disproportionately high mortality and morbidity. Here, we report ultradeep targeted sequencing of a prospective cohort of 237 tumors from 234 patients consisting of both glioblastoma (GBM) and lower-grade glioma (LGG) using our customized gene panels. We identified 2,485 somatic mutations, including single-nucleotide substitutions and small indels, using a validated in-house protocol. Sixty-one percent of the mutations were contributed by 12 hypermutators. The hypermutators were enriched for recurrent tumors and had comparable outcome, and most were associated with temozolomide exposure. *TP53* was the most frequently mutated gene in our cohort, followed by *IDH1* and *EGFR*. We detected at least one *EGFR* mutation in 23% of LGGs, which was significantly higher than 6% seen in The Cancer Genome Atlas, a pattern that can be partially explained by the different patient composition and sequencing depth. *IDH* hotspot mutations were found with higher frequencies in LGG (83%) and secondary GBM (77%) than primary GBM (9%). Multivariate analyses controlling for age, histology, and tumor grade confirm the prognostic value of *IDH* mutation. We predicted 1p/19q status using the panel sequencing data and received only modest performance by benchmarking the prediction to FISH results of 50 tumors. Targeted therapy based on the sequencing data resulted in three responders out of 14 participants. In conclusion, our study suggests ultradeep targeted sequencing can recapitulate previous findings and can be a useful approach in the clinical setting.

Introduction

Malignant gliomas are a group of intracranial tumors associated with disproportionately high mortality and morbidity. The most common and aggressive subtype is grade IV glioblastoma (GBM), which has a dismal median survival of 15 months despite an intrusive standard of care comprising surgery, radiotherapy, and chemotherapy (1). Lower-grade gliomas (LGG, grade II to III) usually have a much better outcome, but they eventually progress to higher grade. Glioma represents one of the most challenging malignancies due to their anatomic location in the brain. Treatment options for glioma have not significantly changed in the past two decades.

Recent genomic profiling efforts such as The Cancer Genome Atlas (TCGA) have revealed the genetic and epigenetic landscape of glioma. Integrated DNA sequencing and copy-number analysis pinpointed potential driver genes including not only known players such as *EGFR*, *TP53*, *IDH1*, *CDKN2A*, etc., but also novel genes such as *LZTR1* and *FGFR-TACC* fusions (2–5). Unsupervised clustering of gene expression and DNA methylation profiles led to the discoveries of three robust transcriptome-based GBM subtypes and a hypermethylation phenotype (G-CIMP) featuring recurrent mutations in *IDH* genes (6, 7). The TCGA pan-glioma analysis identified six methylation subtypes that demonstrate significant overlap with genetic alterations (4). Importantly, multiple groups independently reported a highly consistent genetic classification of LGGs using *IDH* mutations and 1p/19q codeletions (2, 8). In this classification, *IDH* mutations are the top-tier marker that separates LGGs into mutant and wild-type, followed by 1p/19q codeletion as the second marker that further divides mutant tumors. The new World Health Organization classification has incorporated this schema to mitigate variations in pathologic review (9). These advances collectively demonstrate that molecular profiling not only can provide insights into glioma biology but also represents an important tool toward personalized diagnosis and therapeutic interventions for glioma.

Panel sequencing has been tested in the clinical setting for selecting the most probable responders to certain cancer drugs, as the returned results inform on alterations of the targetable genes, mostly established cancer genes, in the tumor. These alterations can be subsequently matched to one or multiple therapeutic

[1]Department of Neuro-Oncology, The University of Texas MD Anderson Cancer Center, Houston, Texas. [2]Department of Genomic Medicine, The University of Texas MD Anderson Cancer Center, Houston, Texas. [3]Department of Epidemiology and Biostatistics, Greehey Children's Cancer Research Institute, The University of Texas Health Science Center at San Antonio, San Antonio, Texas. [4]Department of Biostatistics, The University of Texas MD Anderson Cancer Center, Houston, Texas. [5]Department of Bioinformatics and Computational Biology, The University of Texas MD Anderson Cancer Center, Houston, Texas. [6]Institute of Personalized Cancer Therapy, The University of Texas MD Anderson Cancer Center, Houston, Texas. [7]Department of Pathology, The University of Texas MD Anderson Cancer Center, Houston, Texas. [8]The Jackson Lab for Genomic Medicine, Farmington, Connecticut.

Note: Supplementary data for this article are available at Molecular Cancer Therapeutics Online (http://mct.aacrjournals.org/).

Corresponding Authors: Siyuan Zheng, The University of Texas Health Science Center at San Antonio, San Antonio, TX 78229. Phone: 210-562-9028; Fax: 210-562-9014; E-mail: zhengs3@uthscsa.edu; and John F. de Groot, The University of Texas MD Anderson Cancer Center, 1515 Holcombe Blvd., Unit 431, Houston, TX 77030. Phone: 713-745-3072; Fax: 713-794-4999; E-mail: jdegroot@mdanderson.org

doi: 10.1158/1535-7163.MCT-18-1122

Published OnlineFirst March 29, 2019; DOI: 10.1158/1535-7163.MCT-18-1122

agents, as illustrated in several large-scale clinical sequencing efforts (10–12). Recently, the American Association for Cancer Research (AACR) coordinated with six major cancer centers to release its consortium panel sequencing project Genomics Evidence Neoplasia Information Exchange (GENIE; ref. 13). Similar efforts on childhood cancers such as pediatric glioma and neuroblastoma were also reported (14, 15). These studies laid the foundation for the approval of clinical use of high-throughput sequencing–based gene panels such as the Foundation Medicine panel and Memorial Sloan Kettering IMPACT panel by the FDA.

In this study, we describe our effort on sequencing a cohort of 234 prospectively collected gliomas using the T200 gene panel developed at MD Anderson Cancer Center. Our goal was to test the utility of panel sequencing in predicting glioma prognosis and matching patients to therapeutic agents based on their genetic profiles.

Materials and Methods

Sample and clinical data collection

Collection and analysis of patient samples were approved by the Institutional Review Board at MD Anderson Cancer Center in accordance with U.S. Common Rule. Written-informed consent was obtained from all participating donors. Clinical annotations, including follow-up, were collected by attending oncologists and were deposited into a central electronic patient portal. Tumor slides were reviewed by our pathologist team. An extra nonoverlapping tissue was collected for three tumors in order to assess intratumoral heterogeneity.

Panel sequencing

For each patient, we collected formalin-fixed paraffin-embedded tumor tissues and peripheral blood for sequencing. The inclusion of matched germline DNA allows us to identify somatic mutations with high confidence. Our sequencing protocol was described in detail elsewhere (16, 17). Briefly, DNA was extracted and sheared followed by library preparation using KAPA library preparation kit. After PCR primer removal, we used biotin-labeled probes for capturing target regions. The captured libraries were sequenced on an Illumina HiSeq 2000 machine following the manufacturer's recommendations. The resulting FASTQ file was demultiplexed using CASAVA 1.8.2 with no mismatches.

Mutation and copy-number calling

Fastq files were aligned to hg19 using BWA followed by duplicate reads removal using Picard. Somatic single-nucleotide variation and small indels were called using VarScan2 (18). We called copy-number alteration by comparing sequencing coverages in matched tumor and normal samples normalizing for the total sequencing depth. We defined a gene as H.AMP if its estimated copy number (ECN) was 5, and a gene as H.DEL if its ECN was 0.6. Mutation, copy number, and clinical data are publicly accessible on synapse (syn18410809).

Other analyses

TCGA glioma mutation data were downloaded from a published study (4). The χ^2 test was used to compare mutation prevalence between TCGA and T200. Cox proportional hazard model was used to assess associations between clinical factors and overall survival (OS). Backwards elimination procedure was used to identify final model with only significant factors, starting from factors including histology, age, grade, and extent of resection. Survival analysis was carried out using SAS version 9.4 (SAS Institute). For mutation signature analysis, we counted the types of substitutions as a surrogate for mutation signature instead of applying a deconvolution algorithm because the number of mutations in nonhypermutators were too low, and for hypermutators, there were not sufficient mutations in every transition and transversion group except the dominant type such as C>T. Linear regression was performed using the R package lm. Naïve Bayesian prediction and cross-validation were done using the R packages naivebayes and caret.

Results

Patient cohort and assay overview

We prospectively collected 237 tumor samples and their matched peripheral blood from 234 patients (Table 1). One ganglioglioma case was dropped for further analysis because no somatic mutations were detected. Six grade II or III cases lacked clear evidence of pathologic classification. The remainder of the cohort consisted of 22 oligodendrogliomas, 7 mixed gliomas, 35 astrocytomas, and 164 GBMs. In this study, we grouped the tumors into GBM (grade IV, 72%) and LGG (grades II–III, 28%) for comparison with TCGA. However, an important distinction between our cohort and the TCGA cohort is that 105 of the 234 patients in our cohort were pretreated by a systemic therapy,

Table 1. Summary of patient clinical information; IDH mutation includes both IDH1 and IDH2

Histology	Grade	Cohort size	Median age (range)	Median OS (days)	Median follow-up (days)	IDH mutation
Oligodendroglioma						
	II	10	42 (26–71)	—	478	90.0%
	III	12	40 (19–57)	—	1,546	83.3%
Oligoastrocytoma						
	II	1	36 (N/A)	N/A	357	100.0%
	III	6	36 (31–46)	—	772	100.0%
Astrocytoma						
	II	8	31 (23–48)	—	924	100.0%
	III	27	33 (19–71)	4,135	837	70.4%
GBM						
	Primary	120	58 (19–84)	530	445	9.2%
	Recurrent	22	53 (35–66)	1,603	1,044	9.1%
	Secondary	22	36 (20–68)	3,228	1,588	77.3%
Unclassified						
	II	6	37 (24–43)	—	749	83.3%

Published OnlineFirst March 29, 2019; DOI: 10.1158/1535-7163.MCT-18-1122

whereas all TCGA patients were treatment naïve, i.e., no treatment before surgical resection. Despite a modest sample size, this distinction allows us to examine the effect of systemic treatments on tumor genomic profiles. Overall, high-grade tumors (grades III and IV) tend to have more recurrent samples in our cohort collection (29%) compared with grade II tumors (12%), likely reflecting more aggressive diseases and referral patterns for high stage tumors. Of the 44 recurrent GBMs, 22 had a history of a previous lower-grade lesion and thus were secondary. These secondary GBMs had similar age with LGGs at the time of diagnosis ($P = 0.93$, Wilcox rank-sum test). Mutations in *IDH1* and *IDH2* (collectively referred to as *IDH* hereafter) were found with high prevalence in LGGs (83%) and secondary GBMs (77%) but much less commonly in primary (9%) and recurrent GBMs (9%). The similar frequencies of *IDH* mutation in primary and recurrent GBMs corroborate the contention that these mutations are acquired early in gliomagenesis (19, 20).

We sequenced a list of 202 genes (T200 panel), which were later expanded to 262 (T200.1 panel; Supplementary Table S1). T200 and T200.1 targeted 4,874 and 5,003 exons, covering cancer-associated genes with an emphasis on targetable genes with a total length of 0.9 and 2.0 million base pairs, respectively. The most frequently mutated genes in glioma including *TP53*, *IDH1/2*, *ATRX*, *CDKN2A*, *EGFR*, *NF1*, *NOTCH1*, *PIK3CA*, and *PTEN* were encompassed by both panels. Comparing with a list of 75 computationally determined driver genes from the TCGA pan-glioma study (4), no driver genes mutated in more than 5% of GBM or LGG were omitted in our panel except *FUBP1*, mutations of which were observed in 9% of LGGs. *CIC*, whose mutations were observed in 16% of LGGs, was included in T200.1 but not T200.

We sequenced 204 tumor/blood pairs with T200, 21 pairs with T200.1, and 12 pairs with both panels. For three tumors, we sequenced two nonoverlapping specimens with T200 to evaluate intratumoral heterogeneity. The median depths of coverage on targeted exons were 1,032 for tumor and 781 for normal with T200, 368 for tumor, and 469 for normal with T200.1. We evaluated the consistency of the two panels using the 12 replicates sequenced by both panels. Eighty-five percent of mutations found by T200 were also detected on T200.1. When germline variants were included, this percentage rose to 95%. T200.1 panel generally identified more mutations due to its larger targeted territories, but this difference was not statistically different ($P = 0.4$, Wilcox rank-sum test).

For the three patients for which we sequenced two distinct specimens, in two of them, both specimens yielded the same mutation calls. These two cases included an *IDH* mutant, 1p/19q noncodeletion grade II glioma, and an *IDH* wild-type primary GBM. The last case was also an *IDH* wild-type primary GBM. Interestingly for this case, we detected five mutations in the first specimen and four mutations in the second specimen, and *BRAF* V600E mutation was the only mutation shared between the two specimens (Supplementary Fig. S1). This pattern of limited genetic similarity was reminiscent of branched evolution reported by us and others elsewhere (20, 21). Both specimens harbored mutations in *PTEN*, but the mutations occurred at different loci in distinct forms (missense point mutation vs. a two-nucleotide deletion), suggesting a remarkable selective pressure-driven evolutionary convergence on this important tumor-suppressor gene.

Patterns of cancer gene mutations across glioma groups

We designed and deployed a rigorously tested protocol that automates reads alignment, mutation and indel calling, filtering, and annotation (17). Using this centralized pipeline, we detected a total of 2,485 somatic mutations, including single-nucleotide point mutations and small indels. The vast majority of the mutations cause changes to the encoded protein products, predominantly missense ($n = 2{,}151$, 87%). Only 35 mutations (1.4%) were synonymous, compared with 24% observed in TCGA ($P < 0.05$, t test), suggesting a strong selection for nonsynonymous mutations in the cancer genes sequenced on T200. Tumor suppressors, including *PTEN*, *RB1*, and *ATRX*, were enriched for deactivating mutations such as frameshift indels and gain of stop codons, illustrated by a panel of manually curated driver genes (Fig. 1). The median number of mutations per case was 4 (0–427, SD = 35), but a few cases were evident outliers indicative of a hypermutation phenotype. We examined the distribution of mutational loads and manually selected a cutoff 30 to identify 12 hypermutators (Supplementary Fig. S2). Combined, these 12 samples, which accounted for 5% of the entire cohort, contributed 61% of the total mutations ($n = 1{,}506$).

We next counted the prevalence of genes mutated in our cohort excluding hypermutators (Fig. 2A). *TP53* was the most frequently mutated gene, followed by *IDH*, *EGFR*, and *PTEN*. PI3K pathway genes, including *PIK3CA*, *PIK3CG*, and *PIK3R1*, were collectively mutated in 37 patients (16%), suggesting that targeting this pathway could have important potential in treating glioma. Surprisingly, we found 10 patients harboring *BRAF* mutations, 9 of which were V600E. These patients could potentially benefit from receiving BRAF inhibitors (see below).

Because our samples were collected from various histopathologic subtypes, we compared prevalence of gene mutation across these groups. For this analysis, we initially focused on the 144 genes that were sequenced by both T200 and T200.1. This list allowed us to use all our cases except hypermutators, which were excluded in the comparison. We also excluded genes that were mutated in less than 5% of the cohort because it was challenging to confidently identify group preference with too few mutations, and furthermore, excluding them reduced the multiple testing problem by narrowing search space. Not surprisingly, *ATRX*, *IDH1*, *RB1*, *PTEN*, and *TP53* were all significant, suggesting they were differentially mutated across the groups (FDR < 0.01, Fig. 2B). We verified their significance by repeating the analysis using cases sequenced by T200 only and found one more significant gene, filaggrin (*FLG*), underrepresented in lower-grade tumors (0%). In contrast, it was mutated in around 10% of GBMs, including secondary GBM (11.8%). In TCGA, this gene was mutated in 2% of LGGs but 8% of GBMs (Supplementary Table S1). *FLG* encodes an intermediate filament-associated protein that aggregates keratin intermediate filaments in mammalian epidermis, and it was identified as a significantly mutated gene in esophageal adenocarcinoma (22).

Higher frequency of *EGFR* mutations was previously reported in GBM than LGG (2). We found *EGFR* mutations evenly distributed across the groups. Unlike TCGA that identified *EGFR* mutations in 6% of LGGs, we observed 23% mutation in our cohort (FDR = 1.6e–4, χ^2 test, Fig. 2B). The mutation frequencies were similar in primary GBM between our cohort and TCGA (FDR = 0.32, 26% vs. 19%). We speculate that the elevated prevalence of *EGFR* mutation compared with TCGA in lower-grade tumors might be due to the different composition of patients in the two

Published OnlineFirst March 29, 2019; DOI: 10.1158/1535-7163.MCT-18-1122

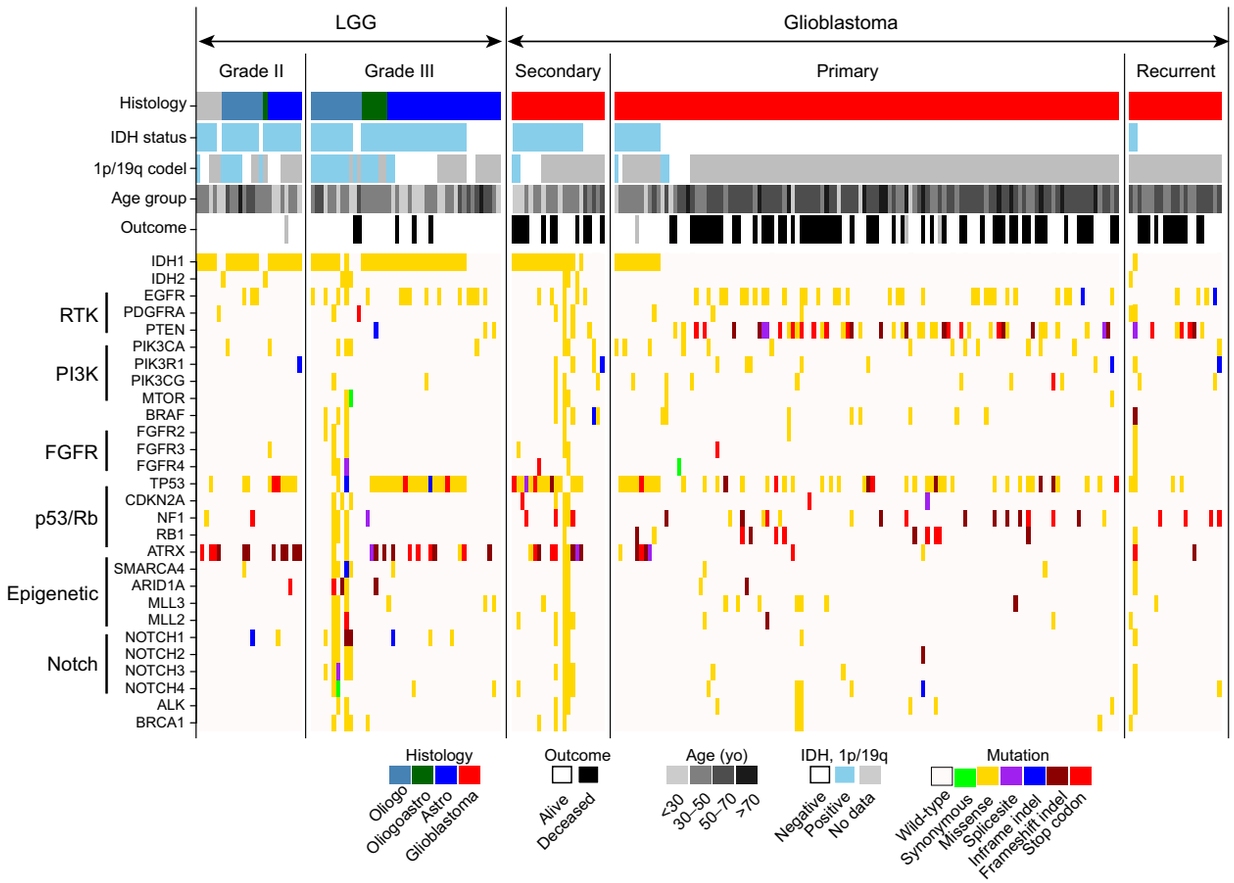

Figure 1.

Landscape of prospective clinical sequencing of 234 gliomas. A list of manually selected genes are grouped into pathways, and their mutations are color coded according to functional consequences on protein products. Clinical and pathohistologic parameters are listed on top of the heatmap.

studies, and the fact that our sequencing data have a higher depth of coverage. Consistent with TCGA, *EGFR* is more frequently amplified in GBM (34%) than LGG (4%) in our dataset.

To gain further insights into the elevated mutation frequency, we compared *EGFR* variant allele fraction (VAF), i.e., the fraction of reads carrying variant allele over the total number of reads, across glioma groups (Fig. 2C). VAFs in astrocytoma and oligodendroglioma, particularly oligodendroglioma, were significantly lower than that in GBM ($P < 0.001$, t test). We speculate that the lower VAFs suggest *EGFR* mutations in these groups were likely present in a small subset of cells. It was unclear if these mutations endowed the carrying cells with growth advantage over other clones.

IDH mutation and 1p/19q codeletion as biomarkers for glioma classification

IDH mutation and 1p/19q codeletion as biomarkers have been adopted in the WHO glioma classification system (9). We tested the utility of T200 panel sequencing as a tool to call these markers. Mutations in *IDH1* and *IDH2* predominantly affect amino acid 132 of IDH1 and the analogous amino acid 172 of IDH2 (23). We detected mutations in *IDH1* or *IDH2* in 88 tumors, including four hypermutators (Table 1). As expected, low-grade gliomas were predominantly *IDH* mutants (83%–100%), compared with grade III astrocytoma (70%) or primary and recurrent GBM (9%). All seven mixed gliomas harbored *IDH* mutations. The 84 nonhypermutators all had only one *IDH* mutation, affecting either R332 in IDH1 or R172 in IDH2. The only exception was a recurrent GBM case where a I98T mutation was found in IDH2. The four hypermutators harbored more than one mutations in *IDH*, but *IDH1* R132H was found in all four with higher VAFs than other *IDH* mutations with borderline significance ($P = 0.15$, t test), suggesting the hotspot mutation was acquired before the hypermutator phenotype.

We examined the prognostic value of *IDH* mutations (Supplementary Table S2 and Supplementary Fig. S3). A univariate analysis using Cox proportional hazard model suggests *IDH* wild-type patients had significantly worse OS than mutants [$P < 0.0001$; HR, 8.8; 95% confidence interval (CI), 4.6–16.8]. A multivariate analysis controlling for tumor grade, pathology, and age confirmed the significant association between *IDH* mutation and better outcome ($P = 0.003$, HR = 0.25).

We sought to determine 1p/19q codeletion status out of the panel sequencing data, though profound noise in copy-number prediction has been noticed previously (24). We compared coverages of captured regions between tumor and normal samples for

Published OnlineFirst March 29, 2019; DOI: 10.1158/1535-7163.MCT-18-1122

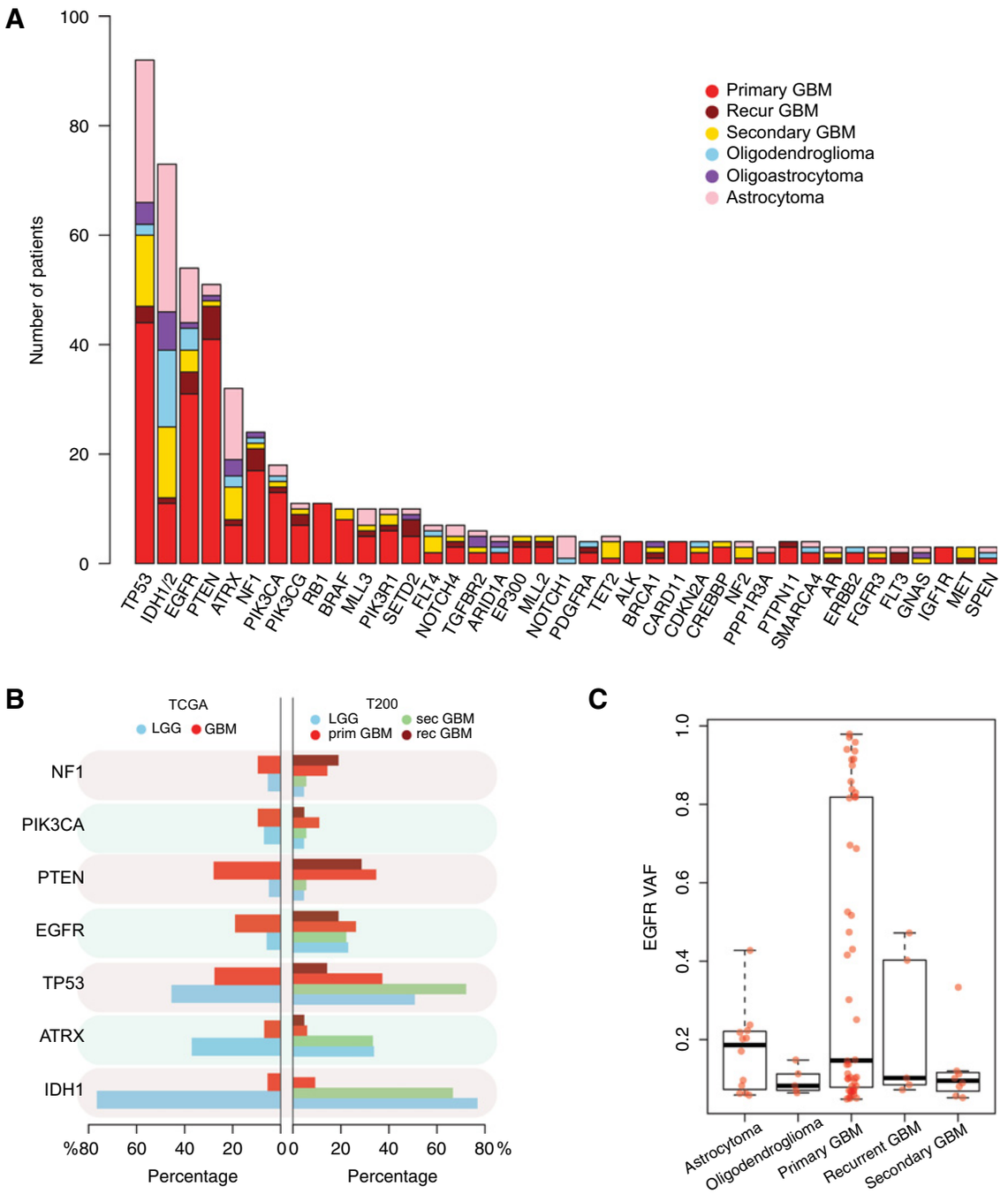

Figure 2.

Mutation prevalence across histologic groups. **A,** A summary of mutations at the gene level across the entire cohort. Genes are sorted by mutation frequency. Hypermutators are excluded. **B,** Glioma genes showing differential distribution across patient groups. Mutation frequency in TCGA is listed side by side for comparison. Note that TCGA does not have recurrent or secondary GBMs. **C,** VAF of EGFR mutations in patient groups.

1p and 19q, correcting for GC content and total sequencing coverage of the sample. We also calculated B allele fraction (BAF) for each capture region. In addition, we performed FISH on 50 cases (35 LGGs and 15 GBMs) to provide a benchmark dataset for this prediction.

As expected, copy-number signal from panel sequencing was noisy, with large variations observed in essentially all chromosome arms tested (Fig. 3A). BAF and copy number of 1p and 19 were positively correlated ($r = 0.64$, $P < 0.001$, Pearson correlation; Fig. 3B), raising the possibility that using 1p or

Published OnlineFirst March 29, 2019; DOI: 10.1158/1535-7163.MCT-18-1122

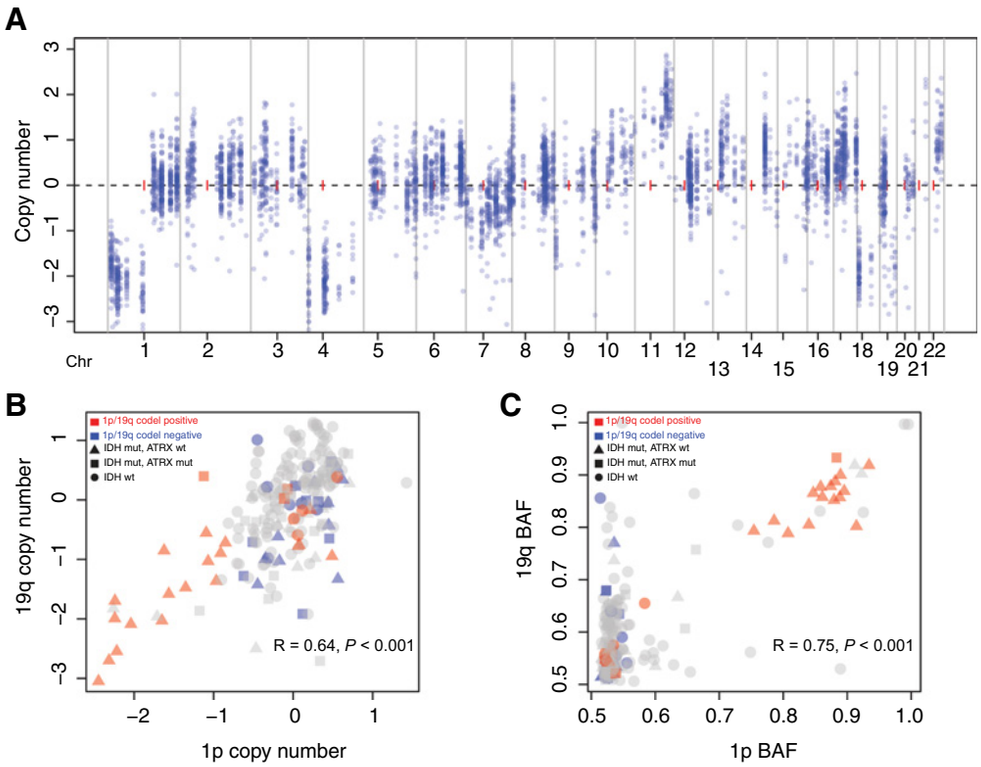

Figure 3.

Prediction of 1p/19q codeletion status. **A,** An example of 1p/19q codeletion–positive case. Each dot represents a capture exon. Copy number at the *y* axis is median centered. **B,** Positive correlation between 1p and 19q copy-number signals. Different shapes of the dots represent different genotype. Red and blue represent 1p/19q codeletion–positive and –negative tumors determined by FISH, respectively. **C,** Similar to **B**, a positive correlation is found between 1p and 19q BAFs. Notably, BAF signals are better separating positive and negative tumors.

19q alone can be sufficient to determine 1p/19q status. We tested this approach by using an empirical threshold for 1p (CN < –0.7 or BAF > 0.7). Benchmarking against FISH data, we obtained a sensitivity of 0.64 and a specificity of 1.0, respectively. The low sensitivity was due to nine cases that demonstrated relatively high copy numbers despite their positive results by FISH (Fig. 3B and C).

We next applied Naïve Bayes classifier considering copy number and BAF of both 1p and 19q as features to predict their status. Leave-one-out cross-validation suggests an accuracy of 0.82 of the model. Nine cases were misclassified, eight of which overlapped with the misclassified cases from the empirical approach. All eight were predicted to be 1p/19q codeletion negative, although FISH data suggested otherwise. Among them, three were *IDH* wild-type, thus molecularly resembling high-grade astrocytoma and GBM. We speculate that FISH was able to capture subtle 1p/19q codeletion signals beyond the resolution of the panel platform. Overall, the modest performance of our data in predicting 1p/19q status was consistent with previous reports (24), raising caution and reiterating the importance of orthogonal validation.

Hypermutation phenotype is more frequent in recurrent lower-grade tumors

Despite the limited coverage offered by targeted sequencing, we observed 12 tumors with excessive mutational load (Supplementary Fig. S2), including five lower-grade tumors (7%), four secondary (18%), two primary (2%), and one recurrent GBMs (5%). All 12 cases received some form of systematic treatment, including radiation, chemo, angiogenesis inhibition, and in some cases, miscellaneous antineoplastic drugs. Seven of the 12 cases demonstrated the temozolomide signature, with C>T substitutions accounting for 95% of all point mutations (Fig. 4A; Supplementary Fig. S4). No evidence of altered polymerase POLE-associated hypermutation (featuring C>A transversion at CpT dinucleotide and C>T transition at CpG dinucleotide) was observed in any of the hypermutators. We note that deconvolution of the mutations into 96 trinucleotide context signatures, as described previously (25), was not successful due to the sparsity of mutations other than C>T. Notably, two secondary GBMs demonstrated almost entirely C>A mutations. C>A mutations are best known to be caused by tobacco consumption and are abundant in lung cancer (25, 26). Retrospectively examining their records, we found that 1 patient was a light smoker, whereas the other was a nonsmoker. More data are warranted to explain what caused the predominant C>A mutation pattern.

We examined mutational load as a function of molecular markers and histologic groups using multivariable linear regression. Interestingly, disease status, i.e., disease at initial diagnosis (primary disease) or recurrence, explained as much variance in mutational load as histology (6% for both), only slightly lower than *ATRX* mutations (7%). When separating tumors into primary and recurrent groups, we found a significant enrichment of

Published OnlineFirst March 29, 2019; DOI: 10.1158/1535-7163.MCT-18-1122

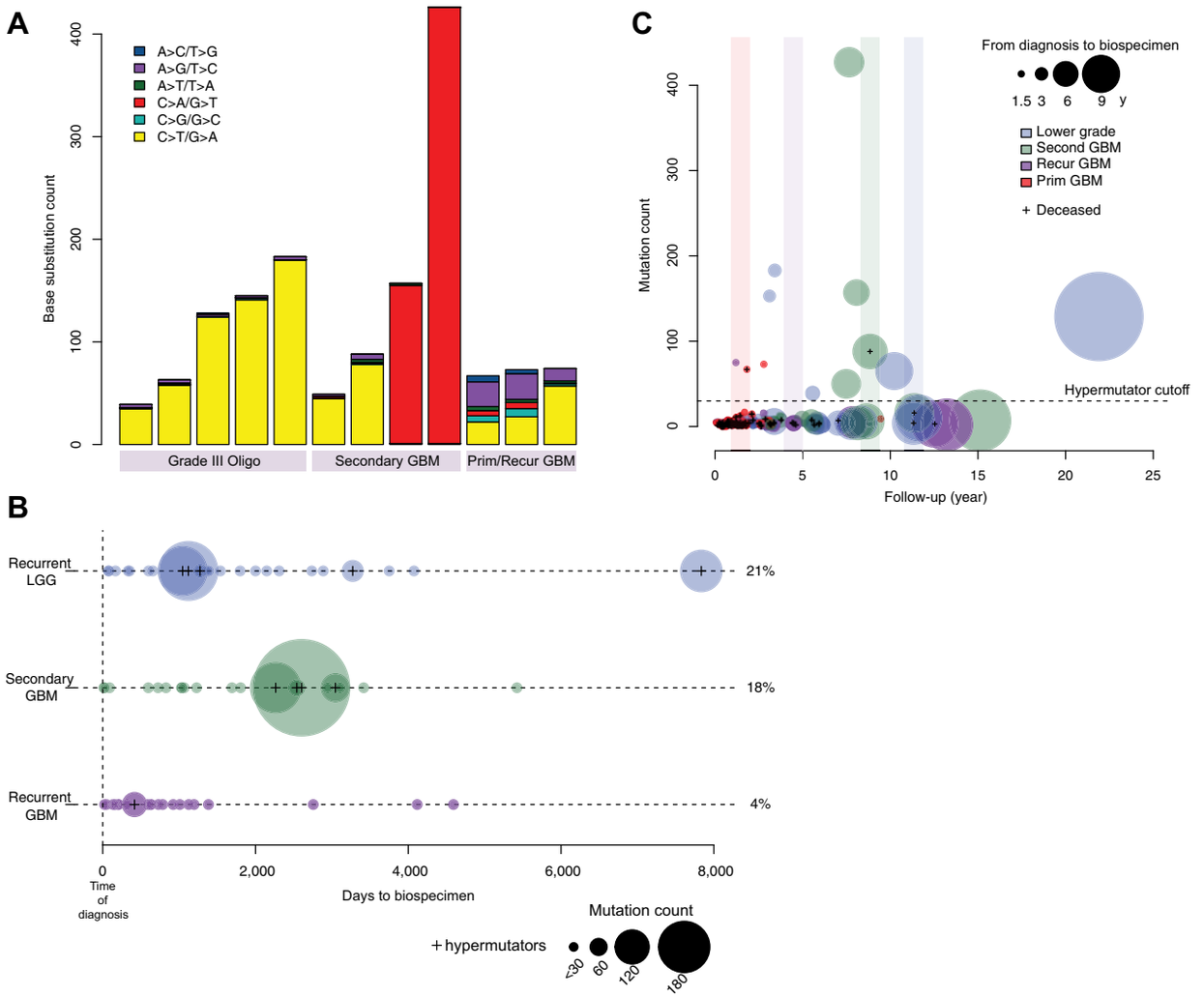

Figure 4.

Mutational and clinical characteristics of hypermutators. **A,** Mutation spectrum of the 12 hypermutators ordered by disease groups. **B,** Mutational load in relation to time window from initial diagnosis to the timepoint when biospecimen was taken. Only recurrent tumors are shown because all primary tumors are essentially resected at the time of diagnosis and thus would cluster around 0. **C,** Mutational load (*y* axis) versus patient outcome (*x* axis, follow-up in years). Node size is proportional to the time from diagnosis to the time when biospecimen was taken. Four color bars indicate the median OS in a window of 400 days. Because the median OS of the lower-grade tumor group has not been reached, we use the lower 95% CI instead.

hypermutators in the recurrent group ($P = 1.2e{-}4$, χ^2 test). For recurrent lower-grade tumors, 21% were hypermutators, compared with none in the primary group. This percentage is similar to secondary GBM (18%) where all tumors by definition were recurrent. In contrast, only 4% of recurrent GBMs were hypermutators. We noticed that hypermutators in recurrent LGGs and secondary GBMs were typically years apart from their initial diagnosis when their tumors were sequenced, much longer than the single recurrent GBM case (Fig. 4B). We were able to collect information on duration of temozolomide treatment for 204 patients. The rest were either treated before being referred to MD Anderson or did not respond to follow-up. Hypermutators received significantly more cycles of temozolomide than nonhypermutators (Wilcoxon rank-sum test, $P = 0.01$), suggesting prolonged exposure to exogenous agents might catalyze the generation of hypermutation phenotype.

We next examined whether hypermutation was associated with outcome in glioma, especially given that a subset of these hypermutators seemed to be caused by chemotherapy (temozolomide) observed here and elsewhere (27). Ten of 12 hypermutators were alive at the latest follow-up, an outcome comparable with the average cases in the respective pathological group ($P = 0.08$, Cox proportional hazard model correcting for pathology and age; HR, 0.16; 95% CI, 0.02–1.2; Fig. 4C). Despite a small sample size, these data suggest increased mutational load did not significantly promote tumor aggressiveness.

Clinical utility for directing targeted therapy

Of the 202 T200 genes, 114 were targetable according to our proprietary Personalized Cancer Therapy knowledge base (http://pct.mdanderson.org). Informed of their tumor profiling results, 14 patients consented for receiving targeted therapeutic agents

Published OnlineFirst March 29, 2019; DOI: 10.1158/1535-7163.MCT-18-1122

and eventually ten received them. These agents included those targeting *PDGFRA*, *BRAF*, *PI3K*, and *IDH* mutations. Of the 10 patients, 3 remained currently on treatment after 38 months (BRAF inhibitor), 21 months (IDH inhibitor), and 35 months (IDH inhibitor). These 3 patients included a recurrent GBM, a grade III oligoastrocytoma, and a grade III oligodendroglioma. Both lower-grade tumors were *IDH* mutants and had a history of disease progression.

The most exceptional responder out of our 10 patients is a 34-year-old female patient. The patient was diagnosed with a primary GBM, for which she underwent a subtotal resection followed by adjuvant concurrent radiation and low-dose temozolomide. After completion of 12 cycles of temozolomide, progressive disease was noted on imaging and was confirmed by biopsy. T200 sequencing revealed the presence of a BRAF V600E mutation in the recurrent tumor. This patient was subsequently treated with the BRAF inhibitor, Dabrafenib, in combination with the MEK inhibitor trametinib. The patient has remained without evidence of progressive disease at the latest follow-up, after the completion of 38 cycles of treatment.

Discussion

In this study, we report target sequencing of 234 gliomas including low- and high-grade, primary, secondary, and recurrent tumors. This broad histopathologic spectrum reflects our intent to recapitulate patient cohort seen in the clinic. Developing upon our institutional efforts, we aimed at addressing two questions: (1) to assess panel sequencing as a prognostic and diagnostic tool in glioma, and (2) to establish a pipeline that could allow us to select glioma patients for clinical trials. Though the genes on the panel were not elected specifically for glioma, our platform included almost all known targetable glioma driver genes. Importantly, some genes that may not be elected for glioma such as *BRAF* were on the pan-cancer panel and proved informative for patient management and outcomes.

Our analysis suggests T200 can recapitulate patterns reported by TCGA and others, most notably histological group associated mutations in glioma genes. These associations can be used in combination with pathologic review to help clarify disease diagnosis. Using prospectively collected tumors, we show that *IDH* mutation is a prognostic marker after adjusting for age, grade, and histology. Predicting 1p/19q status using T200 data yielded only modest performance, especially low sensitivity, reflecting the technical challenge of calling copy-number signals from targeted sequencing. However, the specificity was high, suggesting that when T200 indicates that 1p/19q is lost, it is likely valid. Discrepancies with FISH result, which is commonly regarded as golden standard, indicate that T200 is not yet ready to replace this cytogenetic technique but that it could be used as a preselection approach with only 1p/19q normal on T200 requiring FISH which is a more challenging assay.

The hypermutation phenotype recently received much attention (28, 29), as higher mutational load partially predicts positive response to immune checkpoint blockade (30, 31). We identified 12 hypermutators from our cohort, 7 demonstrated temozolomide-related mutational signature, suggesting cytotoxic agents can serve as potent mutagens. Accordingly, we observed an enrichment of these hypermutators in recurrent tumors. Interestingly, the hypermutators had comparable outcome than nonhypermutators, in fact, slightly better ($P = 0.08$, Cox proportional hazard model, correcting for pathology and age; HR, 0.16; 95% CI, 0.02–1.2), suggesting the additional mutations acquired did not confer significant growth incentive or evolutionary advantage to the tumor. Recent studies suggest excessive somatic mutations may facilitate the generation of more neoantigens and thus elicit stronger immune cell infiltration to the tumor niche, resulting in a more hostile growth environment (32, 33). Nevertheless, these hypermutators could be excellent candidates for immune therapy trials should other clinical options be exhausted.

In gliomas, molecular profiling is not yet mainstream practice as the clinical relevance is still to be determined. In current clinical practice, most treatment decisions for gliomas are largely made based on the patient's age and performance status. However, the recent inclusion of *IDH* mutation and 1p/19q loss into classifiers for gliomas suggests that these do report on patient outcomes. To a large extent despite our growing understanding of the extensive heterogeneity of gliomas, a one-size-fits-all approach is employed. Presently, there are no targeted agents that have led to improved clinical outcomes in gliomas. Overall, single-agent targeted therapy to date has been extremely disappointing due to the inherent heterogeneity of the disease and due to multiple driver mutations in different cell populations within a tumor. Many agents have been developed, but overall response rates continue to be poor with some exceptions such as our 3 patients who have demonstrated durable responses on a biomarker-driven clinical trial. These patients demonstrating longer than expected responses underscore our need to better understand the importance of patient selection and enrichment for clinical trials in order to identify the subset of patients most likely to benefit from treatment. For those patients who do not respond as well to biomarker-driven therapy tailored to the profiling of their tumor, efforts need to be employed to better understand mechanisms of resistance to avoid the pitfall of trials failing time and time again in gliomas.

Moving forward, rational combination therapy may be superior to monotherapy, and consideration will need to be given to combinatorial strategies utilizing immunotherapy, radiotherapy, targeted therapy, antiangiogenic therapy, and/or chemotherapy. Combinatorial strategies will need to be balanced with the potential risk and likelihood of increased toxicity often referred to as "toxic synergy." Future therapeutic strategies in clinical trials should ideally be informed by molecular profiling results and employ combination therapies with targeted drugs to attack subsets of tumor cells harboring different driver mutations while using treatments with less specificity to target cells with passenger and/or secondary mutations.

Disclosure of Potential Conflicts of Interest

F. Meric-Bernstam serves in a consulting/advisory role for Genentech, Inflection Biosciences, Pieris Pharmaceutical, Xencor, Samsung Bioepis, Sumitomo Group, Spectrum Pharmaceuticals, OrigiMed, Aduro Biotech, and Mersana; and has research funding support from Novartis, AstraZeneca, Taiho Pharmaceutical, Genentech, Calithera Biosciences, Debiopharm Group, Bayer, Aileron Therapeutics, PUMA Biotechnology, Cytomx Therapeutics, Jounce Therapeutics, Zymeworks, Curis, Pfizer, eFFECTOR Therapeutics, Abbvie, Daiichi Sankyo, and Guardant Health. R.G. Verhaak owns stock in Pretzel Therapeutics. G.B. Mills is a consultant for AstraZeneca, Catena Pharmaceuticals, Critical Outcome Technologies, ImmunoMET, Ionis, MedImmune, Nuevolution, Pfizer, Precision Medicine, Signalchem Lifesciences, Symphogen, Takeda/Millenium Pharmaceuticals, and Tarveda; owns stock in Catena Pharmaceuticals, ImmunoMET, SignalChem,

Published OnlineFirst March 29, 2019; DOI: 10.1158/1535-7163.MCT-18-1122

Spindletop Ventures, and Tarveda; has licensed technology of an HRD assay to Myriad Genetics; and has research sponsored by Abbvie, Adelson Medical Research Foundation, AstraZeneca, Breast Cancer Research Foundation, Critical Outcome Technologies, Horizon Diagnostics, Illumina, Immuno-MET, Ionis, Karus Therapuetics, Komen Research Foundation, Nanonstring, Ovarian Cancer Research Foundation, Pfizer, Prospect Creek Foundation, Takeda/Millenium Pharmaceuticals, and Tesaro. W.K.A. Yung is a paid consultant for DNATrix and NBTS and receives honoraria from DNATrix and NBTS. J.F. de Groot has research support from Sanofi-Aventis, AstraZeneca, EMD-Serono, Eli Lilly, Novartis, Deciphera Pharmacetuicals, and Mundipharma; is a paid consultant for Celldex, Deceiphera Pharmaceuticals, Abbvie, FivePrime Therapuetics Inc., GW Pharma, CArthera, Eli Lilly, Boston Biomedical Inc., Kairos Venture Investments, Syneos Health, and Monteris; serves on the advisory board for Genentech, Celldex, Foundation Medicine, Inc., Novogen, Deciphera, AstraZeneca, Insys Therapeutics, Kadmon, Merck, and Eli Lilly; and owns stock in Ziopharm Oncology and Gilead. J.F. de Groot's spouse is employed by Ziopharm Oncology. No potential conflicts of interest were disclosed by the other authors.

Authors' Contributions

Conception and design: G.B. Mills, W.K.A. Yung, J.F. de Groot
Development of methodology: S. Zheng, K. Chen
Acquisition of data (provided animals, acquired and managed patients, provided facilities, etc.): K. Alfaro-Munoz, A.K. Eterovic, K.R.M. Shaw, F. Meric-Bernstam, G.N. Fuller, W.K.A. Yung, S.-P. Weathers, J.F. de Groot
Analysis and interpretation of data (e.g., statistical analysis, biostatistics, computational analysis): S. Zheng, W. Wei, X. Wang, F. Wang, A.K. Eterovic, K. Chen, R.G. Verhaak, G.B. Mills, W.K.A. Yung, S.-P. Weathers, J.F. de Groot
Writing, review, and/or revision of the manuscript: S. Zheng, K. Alfaro-Munoz, W. Wei, F. Meric-Bernstam, G.N. Fuller, G.B. Mills, S.-P. Weathers, J.F. de Groot
Administrative, technical, or material support (i.e., reporting or organizing data, constructing databases): K. Alfaro-Munoz, K.R.M. Shaw, K. Chen
Study supervision: S. Zheng, K. Chen, J.F. de Groot

Acknowledgments

We thank all patients who donated their samples to this project. This work is funded by Sheikh Khalifa Bin Zayed al Nahyan Institute for Personalized Cancer Therapy (IPCT) and Khalifa Bin Zayed Al Nahyan Foundation Grant (F. Meric-Bernstam, K.R.M. Shaw), MD Anderson Glioblastoma Moonshots Program (J.F. de Groot), Marnie Rose Foundation (J.F. de Groot), and Naz Moez Sarrafzadeh Glioma Research Account (W.K.A. Yung). S. Zheng is supported by CPRIT (RR170055) and a Career Enhancement Award of the Brain SPORE at MD Anderson (P50 CA127001).

The costs of publication of this article were defrayed in part by the payment of page charges. This article must therefore be hereby marked *advertisement* in accordance with 18 U.S.C. Section 1734 solely to indicate this fact.

Received September 29, 2018; revised December 18, 2018; accepted March 12, 2019; published first March 29, 2019.

References

1. Dunn GP, Rinne ML, Wykosky J, Genovese G, Quayle SN, Dunn IF, et al. Emerging insights into the molecular and cellular basis of glioblastoma. Genes Dev 2012;26:756–84.
2. Cancer Genome Atlas Research Network, Brat DJ, Verhaak RG, Aldape KD, Yung WK, Salama SR, et al. Comprehensive, integrative genomic analysis of diffuse lower-grade gliomas. N Engl J Med 2015;372:2481–98.
3. Frattini V, Trifonov V, Chan JM, Castano A, Lia M, Abate F, et al. The integrated landscape of driver genomic alterations in glioblastoma. Nat Genet 2013;45:1141–9.
4. Ceccarelli M, Barthel FP, Malta TM, Sabedot TS, Salama SR, Murray BA, et al. Molecular profiling reveals biologically discrete subsets and pathways of progression in diffuse glioma. Cell 2016;164:550–63.
5. Singh D, Chan JM, Zoppoli P, Niola F, Sullivan R, Castano A, et al. Transforming fusions of FGFR and TACC genes in human glioblastoma. Science 2012;337:1231–5.
6. Wang Q, Hu B, Hu X, Kim H, Squatrito M, Scarpace L, et al. Tumor evolution of glioma-intrinsic gene expression subtypes associates with immunological changes in the microenvironment. Cancer Cell 2017;32:42–56e6.
7. Noushmehr H, Weisenberger DJ, Diefes K, Phillips HS, Pujara K, Berman BP, et al. Identification of a CpG island methylator phenotype that defines a distinct subgroup of glioma. Cancer Cell 2010;17:510–22.
8. Eckel-Passow JE, Lachance DH, Molinaro AM, Walsh KM, Decker PA, Sicotte H, et al. Glioma groups based on 1p/19q, IDH, and TERT promoter mutations in tumors. N Engl J Med 2015;372:2499–508.
9. Louis DN, Perry A, Reifenberger G, von Deimling A, Figarella-Branger D, Cavenee WK, et al. The 2016 world health organization classification of tumors of the central nervous system: a summary. Acta Neuropathologica 2016;131:803–20.
10. Zehir A, Benayed R, Shah RH, Syed A, Middha S, Kim HR, et al. Mutational landscape of metastatic cancer revealed from prospective clinical sequencing of 10,000 patients. Nat Med 2017;23:703–13.
11. Jordan EJ, Kim HR, Arcila ME, Barron D, Chakravarty D, Gao J, et al. Prospective comprehensive molecular characterization of lung adenocarcinomas for efficient patient matching to approved and emerging therapies. Cancer Discov 2017;7:596–609.
12. Abida W, Armenia J, Gopalan A, Brennan R, Walsh M, Barron D, et al. Prospective genomic profiling of prostate cancer across disease states reveals germline and somatic alterations that may affect clinical decision making. JCO Precis Oncol 2017;2017.
13. Consortium APG. AACR Project GENIE: powering precision medicine through an international consortium. Cancer Discov 2017;7:818–31.
14. Ramkissoon SH, Bandopadhayay P, Hwang J, Ramkissoon LA, Greenwald NF, Schumacher SE, et al. Clinical targeted exome-based sequencing in combination with genome-wide copy number profiling: precision medicine analysis of 203 pediatric brain tumors. Neuro-oncology 2017;19:986–96.
15. Lee SH, Kim JS, Zheng S, Huse JT, Bae JS, Lee JW, et al. ARID1B alterations identify aggressive tumors in neuroblastoma. Oncotarget 2017;8:45943–50.
16. Meric-Bernstam F, Brusco L, Shaw K, Horombe C, Kopetz S, Davies MA, et al. Feasibility of large-scale genomic testing to facilitate enrollment onto genomically matched clinical trials. J Clin Oncol 2015;33:2753–62.
17. Chen K, Meric-Bernstam F, Zhao H, Zhang Q, Ezzeddine N, Tang LY, et al. Clinical actionability enhanced through deep targeted sequencing of solid tumors. Clinical chemistry 2015;61:544–53.
18. Koboldt DC, Zhang Q, Larson DE, Shen D, McLellan MD, Lin L, et al. VarScan 2: somatic mutation and copy number alteration discovery in cancer by exome sequencing. Genome Res 2012;22:568–76.
19. Johnson BE, Mazor T, Hong C, Barnes M, Aihara K, McLean CY, et al. Mutational analysis reveals the origin and therapy-driven evolution of recurrent glioma. Science 2014;343:189–93.
20. Kim H, Zheng S, Amini SS, Virk SM, Mikkelsen T, Brat DJ, et al. Whole-genome and multisector exome sequencing of primary and post-treatment glioblastoma reveals patterns of tumor evolution. Genome Res 2015;25:316–27.
21. Kim J, Lee IH, Cho HJ, Park CK, Jung YS, Kim Y, et al. Spatiotemporal evolution of the primary glioblastoma genome. Cancer Cell 2015;28:318–28.
22. Lawrence MS, Stojanov P, Mermel CH, Robinson JT, Garraway LA, Golub TR, et al. Discovery and saturation analysis of cancer genes across 21 tumour types. Nature 2014;505:495–501.
23. Yan H, Parsons DW, Jin G, McLendon R, Rasheed BA, Yuan W, et al. IDH1 and IDH2 mutations in gliomas. N Engl J Med 2009;360:765–73.
24. Rieber N, Bohnert R, Ziehm U, Jansen G. Reliability of algorithmic somatic copy number alteration detection from targeted capture data. Bioinformatics 2017;33:2791–8.
25. Alexandrov LB, Nik-Zainal S, Wedge DC, Aparicio SA, Behjati S, Biankin AV, et al. Signatures of mutational processes in human cancer. Nature 2013;500:415–21.

Published OnlineFirst March 29, 2019; DOI: 10.1158/1535-7163.MCT-18-1122

26. Lawrence MS, Stojanov P, Polak P, Kryukov GV, Cibulskis K, Sivachenko A, et al. Mutational heterogeneity in cancer and the search for new cancer-associated genes. Nature 2013;499:214–8.
27. Johnson BE, Mazor T, Hong C, Barnes M, Aihara K, McLean CY, et al. Mutational analysis reveals the origin and therapy-driven evolution of recurrent glioma. Science 2014;343:189–93.
28. Campbell BB, Light N, Fabrizio D, Zatzman M, Fuligni F, de Borja R, et al. Comprehensive analysis of hypermutation in human cancer. Cell 2017; 171:1042–56.e10.
29. Bailey MH, Tokheim C, Porta-Pardo E, Sengupta S, Bertrand D, Weerasinghe A, et al. Comprehensive characterization of cancer driver genes and mutations. Cell 2018;174:1034–5.
30. Van Allen EM, Miao D, Schilling B, Shukla SA, Blank C, Zimmer L, et al. Genomic correlates of response to CTLA-4 blockade in metastatic melanoma. Science 2015;350:207–11.
31. Yarchoan M, Hopkins A, Jaffee EM. Tumor mutational burden and response rate to PD-1 inhibition. N Engl J Med 2017;377: 2500–1.
32. Nebot-Bral L, Brandao D, Verlingue L, Rouleau E, Caron O, Despras E, et al. Hypermutated tumours in the era of immunotherapy: the paradigm of personalised medicine. Eur J Cancer 2017;84:290–303.
33. Finocchiaro G, Langella T, Corbetta C, Pellegatta S. Hypermutations in gliomas: a potential immunotherapy target. Discov Med 2017;23: 113–20.

AACR American Association for Cancer Research

Molecular Cancer Therapeutics

Prospective Clinical Sequencing of Adult Glioma

Siyuan Zheng, Kristin Alfaro-Munoz, Wei Wei, et al.

Mol Cancer Ther 2019;18:991-1000. Published OnlineFirst March 29, 2019.